The Astrophysical Journal Letters, 771:L6 (5pp), 2013 July 1 doi:10.1088/2041-8205/771/1/L6

DEEP LBT/LUCI SPECTROSCOPY OF AN Lyα EMITTER CANDIDATE AT $z \simeq 7.7$*

Linhua Jiang[1,4], Fuyan Bian[2], Xiaohui Fan[2], Hannah B. Krug[3], Ian D. McGreer[2], Daniel P. Stark[2,4], Benjamin Clément[2], and Eiichi Egami[2]
[1] School of Earth and Space Exploration, Arizona State University, Tempe, AZ 85287-1504, USA; linhua.jiang@asu.edu
[2] Steward Observatory, University of Arizona, 933 North Cherry Avenue, Tucson, AZ 85721, USA
[3] Department of Astronomy, University of Maryland, College Park, MD 20742, USA
Received 2013 April 29; accepted 2013 May 21; published 2013 June 12

ABSTRACT

We present deep spectroscopic observations of an Lyα emitter (LAE) candidate at $z \simeq 7.7$ using the infrared spectrograph LUCI on the 2×8.4 m Large Binocular Telescope (LBT). The candidate is the brightest among the four $z \simeq 7.7$ LAE candidates found in a narrowband imaging survey by Krug et al. Our spectroscopic data include a total of 7.5 hr of integration with LBT/LUCI and are deep enough to significantly (3.2σ–4.9σ) detect the Lyα emission line of this candidate based on its Lyα flux 1.2×10^{-17} erg s^{-1} cm^{-2} estimated from the narrowband photometry. However, we do not find any convincing signal at the expected position of its Lyα emission line, suggesting that this source is not an LAE at $z \simeq 7.7$. The non-detection in this work, together with the previous studies of $z \simeq 7.7$ LAEs, puts a strong constraint on the bright-end Lyα luminosity function (LF) at $z \simeq 7.7$. We find a rapid evolution of the Lyα LF from $z \simeq 6.5$ to 7.7: the upper limit of the $z \simeq 7.7$ LF is more than five times lower than the $z \simeq 6.5$ LF at the bright end ($f \geqslant 1.0 \times 10^{-17}$ erg s^{-1} cm^{-2} or $L \geqslant 6.9 \times 10^{42}$ erg s^{-1}). This is likely caused by an increasing neutral fraction in the intergalactic medium that substantially attenuates Lyα emission at $z \simeq 7.7$.

Key words: cosmology: observations – galaxies: evolution – galaxies: high-redshift

Online-only material: color figure

1. INTRODUCTION

During the epoch of cosmic reionization, the intergalactic medium (IGM) was ionized by the first astrophysical objects, and the universe became transparent to UV photons. Measurements of cosmic microwave background polarization (Komatsu et al. 2011) and studies of high-redshift quasars (Fan et al. 2006) have shown that reionization began earlier than $z \sim 10$ and ended by $z \sim 6$. The process of reionization is complex, and it is still not clear how and when it exactly occurred. Early observational studies were mostly based on high-redshift luminous quasars (e.g., Mesinger & Haiman 2007; Carilli et al. 2010; McGreer et al. 2011). In recent years, as the number of galaxies found at $z \geqslant 6$ has increased dramatically, high-redshift galaxies have begun to play an important role in the study of reionization.

In the last decade, a large number of Lyα emitters (LAEs) and Lyman-break galaxies (LBGs) at $z \geqslant 6$ were discovered using two complementary methods: the narrowband technique and the dropout technique, respectively. In particular, the narrowband (or Lyα) technique has a high success rate of spectroscopic confirmation. Three atmospheric windows with little emission from OH skylines in the optical are often used to search for galaxies at $z \simeq 5.7$, 6.5, and 7. Thus far more than 200 LAEs have been spectroscopically confirmed at these redshifts (e.g., Taniguchi et al. 2005; Iye et al. 2006; Shimasaku et al. 2006; Hu et al. 2010; Ouchi et al. 2010; Kashikawa et al. 2011; Rhoads et al. 2012). Furthermore, a $z \simeq 7.22$ LAE was confirmed recently (Shibuya et al. 2012), demonstrating the ability to detect distant galaxies with powerful ground-based telescopes.

Individual galaxies are usually too faint to provide useful information about the IGM ionization state during the reionization era. However, much can be learned from their statistical properties, such as the evolution of the Lyα luminosity function (LF) and the fraction of galaxies with strong Lyα emission lines among LBGs (e.g., Kashikawa et al. 2011; Stark et al. 2011; Treu et al. 2012). For example, recent studies have shown that the Lyα LF evolves rapidly from $z \sim 5.7$ to 6.5 (Hu et al. 2010; Ouchi et al. 2010; Kashikawa et al. 2011), while the evolution of the LAE UV LF is far less severe. This was explained by the increasing neutral fraction of the IGM from $z \sim 5.7$ to 6.5 that attenuates Lyα emission via resonant scattering of Lyα photons. As such, one would expect a further decline of the Lyα LF at $z > 6.5$. Although the $z \sim 7$ LF has not been well determined due to the limited number of LAEs known at $z \sim 7$, the current data do seem to indicate such an evolutionary trend (Ota et al. 2012; Shibuya et al. 2012).

The narrowband technique is now being used to search for higher redshift LAEs at $z \simeq 7.7$ (e.g., Hibon et al. 2010; Tilvi et al. 2010; Clément et al. 2012; Krug et al. 2012). This redshift corresponds to an OH-dark window at ~1.06 μm in the near-IR. Each of these narrowband surveys, except the one by Clément et al. (2012), found several candidates. Surprisingly, they also found that the Lyα LFs at $z \simeq 7.7$ derived from their photometric samples are consistent with the LF at $z \simeq 6.5$. On the other hand, none of their LAE candidates have been spectroscopically confirmed. Spectroscopic identification of these objects is very challenging, but is critical for understanding the properties of LAEs and the IGM state during reionization. In this Letter, we present deep LBT/LUCI spectroscopy of a $z \simeq 7.7$ LAE

* The LBT is an international collaboration among institutions in the United States, Italy, and Germany. LBT Corporation partners are: The University of Arizona on behalf of the Arizona University system; Istituto Nazionale di Astrofisica, Italy; LBT Beteiligungsgesellschaft, Germany, representing the Max-Planck Society, the Astrophysical Institute Potsdam, and Heidelberg University; The Ohio State University, and The Research Corporation, on behalf of The University of Notre Dame, University of Minnesota, and University of Virginia.
[4] Hubble Fellow.

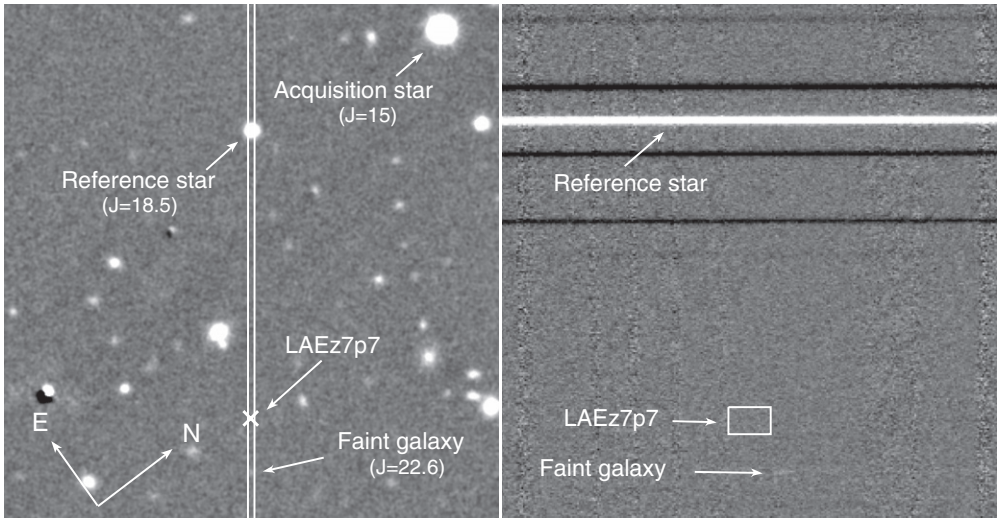

Figure 1. Left: deep J-band image of the LAEz7p7 field from Krug et al. (2012). The position of LAEz7p7 is marked by the cross. With a position angle of 53.°08, the long slit simultaneously covered LAEz7p7, the reference star RefStar ($J_{\rm Vega} = 18.5$), and a very faint galaxy ($J_{\rm Vega} = 22.6$ mag). Right: part of the combined 2D spectrum (1.026–1.083 μm) from LBT/LUCI. We clearly detect the line and continuum emission for the faint galaxy. The box is centered at 1.056 μm, with a size of 50 Å by 4″. The Lyα emission line of LAEz7p7 is expected to be in the middle of the box. However, we do not see any sign of detection. The central part of the box is zoomed in Figure 3(e).

candidate found by Krug et al. (2012). In Section 2, we describe our observations and data reduction. We then present our results in Section 3, and discuss the results in Section 4. We use a Λ-dominated flat cosmology with $H_0 = 70$ km s^{-1} Mpc^{-1}, $\Omega_m = 0.3$, and $\Omega_\Lambda = 0.7$.

2. OBSERVATIONS AND DATA REDUCTION

Our target (hereafter LAEz7p7) is an LAE candidate at $z \simeq 7.7$ selected from Krug et al. (2012), who carried out a deep imaging survey of $z \simeq 7.7$ LAEs with two ultra narrowband filters centered at 1.056 and 1.063 μm. The filter width is ~8 Å. The survey volume is 2.8×10^4 Mpc^3, and the depth is 22.4 AB mag (50% completeness) in the narrow band, corresponding to a Lyα flux limit of 0.8×10^{-17} erg s^{-1} cm^{-2}. They found four candidates down to the survey limit in the two bands. LAEz7p7 is the brightest one (21.87 AB mag in the 1.056 μm band) with an expected Lyα flux of $(1.21 \pm 0.16) \times 10^{-17}$ erg s^{-1} cm^{-2}.

We observed LAEz7p7 using the infrared spectrograph LUCI (Ageorges et al. 2010) on the 2 × 8.4 m Large Binocular Telescope (LBT) on 2012 December 11 and 2013 March 4 (UT). The observing conditions were good, with mostly clear sky and decent seeing (0.″6–0.″9). The observations were made in long-slit mode with a 1″ slit. We did a blind offset from a bright star to LAEz7p7. The long slit had a position angle of 53.°08 so that it covered another nearby star with $J_{\rm Vega} = 18.5$ mag. This star (hereafter RefStar) is used as a reference object (and as a standard star for flux calibration) during the data reduction. The left panel of Figure 1 shows the positions of these objects in the LAEz7p7 field. We chose to use the second order of the 200 H+K grating with a wavelength coverage of ~4000 Å centered at 1.1 μm. This provides a resolving power $R \sim 1000$. The exposure time for each science image was 900 s. The individual exposures were dithered along the slit. The total integration time was 7.5 hr. We also observed a standard star UKIRT FS128 with the same configuration for the purpose of flux calibration.

We reduced the LUCI data using standard methods based on our own customized pipeline (Bian et al. 2010). The basic procedure is as follows. For each raw science image, we first generated a two-dimensional (2D) wavelength map using many OH skylines in the image. The closest dithered neighboring frame was then subtracted from this image. This step removed the dark current and some instrument-related artifacts, and also performed the first sky subtraction. Next, the image was flat-fielded by a master flat image that was made from a series of flat images taken in the same night. A more accurate sky subtraction was performed with the Kelson (2003) algorithm. Finally, we rectified the reduced 2D images (raw images were curved) and interpolated them onto a uniform rectangular output wavelength grid based on the individual 2D wavelength maps.

Before we stacked these images, we shifted them along the spatial direction so that the bright RefStar has the same position in all the images. The accurate position of RefStar in each image was determined by fitting a Gaussian profile to the average flux profile along the spatial direction. The images were then weighted on a frame-by-frame basis by sky transparency, seeing, and background variance. The transparency was measured by the relative flux of RefStar. The variation of the transparency during the same run was very small (a few percent). Seeing was measured as the FWHM of the point-spread function (PSF) from RefStar. The variance of background was calculated around the expected position of LAEz7p7. A final combined 2D image was created by stacking the weighted science images with a sigma (5σ) rejection. The PSF FWHM of RefStar in the stacked image is 0.″7, well consistent with those in input images.

3. RESULTS

Our main result is that we do not detect any convincing signal at the expected position of the LAEz7p7 Lyα emission line in our stacked spectroscopic image. As we will see, this image is deep enough to detect LAEz7p7 at a significance level of 3.2σ–4.9σ if it is a $z \sim 7.7$ LAE with the expected Lyα flux given by Krug et al. (2012). In Figure 1, the right panel shows part of the stacked spectroscopic image. With the known pixel scale (0.″249) and wavelength map, the expected position of LAEz7p7 in the 2D image is accurately determined. This position is in the middle of the box in the right panel. The box covers a range of 50 Å centered at 1.056 μm. A zoomed-in version is shown in Figure 3(e), and the extracted one-dimensional (1D) spectrum

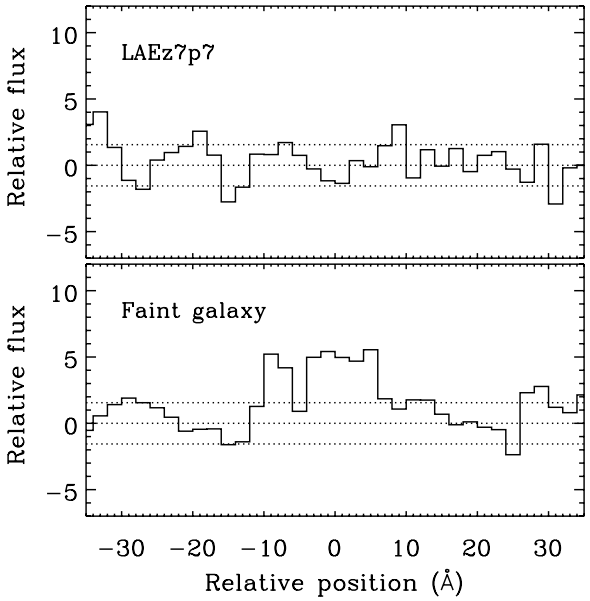

Figure 2. One-dimensional spectra of LAEz7p7 and the faint galaxy. The spectra are extracted within a 5 pixel (1.″25) window using IRAF task `apall`. The dotted lines represent zero flux and 1σ deviation. The spectrum of LAEz7p7 is centered at 1.056 μm and does not show any significant signal. The spectrum of the faint galaxy is centered at 1.060 μm (as indicated in the right panel of Figure 1) and shows a strong detection.

is given in Figure 2. A close visual inspection shows that there is no sign of any significant detection at this position.

We determine the absolute flux calibration using the standard star and RefStar. Their 1D spectra are extracted within a 7 pixel (1.″75) window using IRAF task `apall`. The standard star UKIRT FS128 is an M5V star with $J_{\rm Vega} = 13.00$ mag. The system response curve is derived by comparing the observed spectrum of FS128 with the model spectrum of an M5V star. The spectrum of RefStar is corrected with the response curve and scaled to match its *J*-band photometry. The flux calibration (or conversion between counts and flux) derived from the two stars is consistent with each other (<0.15 mag), indicating that RefStar (and thus LAEz7p7) was placed in the middle of the slit. We calculate the background variance around the expected position of LAEz7p7, and convert it to a 1σ detection per pixel using the absolute flux calibration. This 1σ limit is used to estimate the detection limit of our image. In order to do so, we generate a 2D model Lyα spectrum for LAEz7p7 based on the 1D composite spectrum of $z \simeq 6.5$ LAEs given by Kashikawa et al. (2011). The model spectrum has the same pixel scale as our image. Its PSF FWHM is also 0.″7. When extracted to 1D spectrum, the model spectrum has the shape of the composite $z \simeq 6.5$ spectrum. The model spectrum is shown in Figure 3(a).

The detection significance of a line depends on the number of pixels extracted. We calculate it in a box of 8 Å (the filter width) by 1″ (4 pixels). Based on the 1σ limit derived above, we find that a line with 1.21×10^{-17} erg s^{-1} cm^{-2} should be detected at a 4.9σ level at its expected position in our image. Another way to estimate the detection limit is commonly used for detecting faint objects in 2D imaging data. We assume that the model LAE is detected at $\geqslant$1.5σ in each of five contiguous pixels (the five brightest pixels here). In this case, we expect a 3.2σ detection for LAEz7p7. This limit (3.2σ) is lower than 4.9σ derived above. This is due to the low resolution and good seeing, which cause the flux to be highly concentrated in the central pixels.

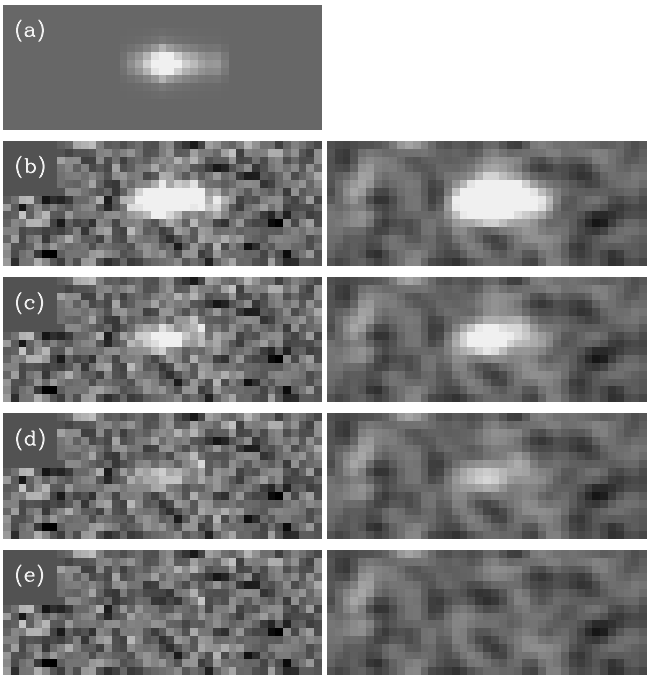

Figure 3. Lyα emission lines of a model LAE at the expected position of LAEz7p7 in our 2D spectroscopic image. Panel (a) shows the model LAE. Panel (e) shows the expected position of LAEz7p7 (the central part of the box in Figure 1). The model line is scaled to be five, two, and one times the estimated Lyα flux of LAEz7p7. The scaled lines are then placed at the expected position. The results are shown in (b), (c), and (d). The images on the right-hand side are the Gaussian-smoothed version (with $\sigma = 1$ pixel) of the images on the left-hand side. It is clear that we are able to visually identify LAEz7p7 if its Lyα emission is as strong as expected.

Visual inspection is another powerful way to identify faint objects. We scale the model LAE and place it at the expected position of LAEz7p7. We then check whether we are able to identify it. The results are shown in Figure 3. Panel (e) shows the expected position of LAEz7p7, i.e., the central part of the box in Figure 1. The model Lyα line is scaled to be five, two, and one times the estimated Lyα flux of LAEz7p7. The scaled spectra are placed at the expected position, shown in panels (b), (c), and (d), respectively. The images on the right-hand side are the Gaussian-smoothed images. The figure demonstrates that LAEz7p7 can be clearly identified if its Lyα emission line is as strong as the value given by Krug et al. (2012). In fact, if LAEz7p7 is a real LAE, its Lyα flux is likely higher than this value, because the 1.056 μm filter is very narrow, and is very likely to only cover part of the Lyα line.

We emphasize that the LAEz7p7 nominal position during our observations was securely located within the slit, with minimum slit losses owing to excellent seeing. This is ensured by two facts. One is the consistency of the flux calibration between RefStar and the standard star, as we discussed earlier. The other fact is the detection of a very faint galaxy ($J_{\rm Vega} = 22.6$ mag) in the same slit. This object was well aligned with LAEz7p7 and RefStar, and was serendipitously covered by the slit (faint galaxy in Figures 1 and 2). We detect both line and continuum emission for the galaxy. This ensures that LAEz7p7 was in the middle of the slit. In addition, the detection of such a faint object (Figure 2) indicates that the image depth is very good.

4. DISCUSSION

With our deep LBT/LUCI spectroscopy, we have ruled out the existence of a strong emission line at $\lambda \sim 1.056$ μm in

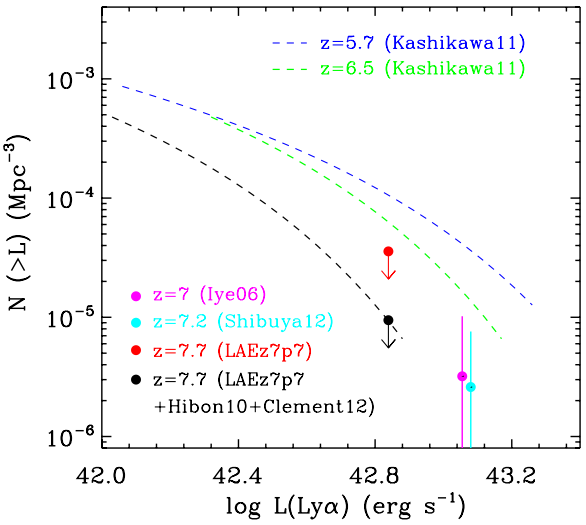

Figure 4. Observed Lyα LFs at high redshift. The dashed blue and green lines represent the LFs at $z \simeq 5.7$ and 6.5 from Kashikawa et al. (2011). The luminosity coverage of the two lines reflects the actual luminosity coverage in their sample. The magenta and cyan circles represent the LFs at $z \simeq 7$ and 7.2, respectively (Iye et al. 2006; Shibuya et al. 2012). The red and black circles indicate the upper limits of the bright-end LF at $z \simeq 7.7$, derived from the non-detection of LAEz7p7 and from the combination of this work and previous studies (Hibon et al. 2010; Clément et al. 2012). The black dashed line shows the evolved $z \simeq 6.5$ LF matched to the upper limit of the $z \simeq 7.7$ LF (black circle). The figure shows a strong evolution of the Lyα LF at the bright end from $z \simeq 6.5$ to 7.7.

(A color version of this figure is available in the online journal.)

LAEz7p7, although this is not sufficient for us to fully explain the nature of this object. The photometric samples of $z \simeq 7.7$ LAEs (and all other high-redshift galaxies), especially those with single-band detections, could be contaminated by various interlopers, such as low-redshift red or dusty galaxies, Galactic late-type dwarf stars, variable (or transient) objects, and even noise spikes. The contamination in LAE samples has been discussed in the previously mentioned LAE papers (also see, e.g., Pirzkal et al. 2013). Because of the rarity of $z \simeq 7.7$ galaxies, even if the vast majority of contaminants can be removed with careful selection, a tiny fraction of them could dominate a sample, highlighting the importance of spectroscopic follow-up observations.

The non-detection of LAEz7p7 allows us to put a constraint on the bright-end Lyα LF at $z \simeq 7.7$. The Krug et al. (2012) survey has a volume of 2.8×10^4 Mpc^3, and found one candidate LAE (LAEz7p7) with Lyα flux higher than 10^{-17} erg s^{-1} cm^{-2}. This translates to an upper limit of the spatial density at the bright end ($L \geqslant 6.9 \times 10^{42}$ erg s^{-1}). Figure 4 shows the upper limit (red circle) compared to previous results. The dashed blue and green lines illustrate the strong decline of the bright-end Lyα LF from $z \simeq 5.7$ to 6.5 (Kashikawa et al. 2011). This has been explained by an increasing neutral fraction of the IGM. As such, we expect to see further decline of the Lyα LF toward higher redshift. The constraints from the $z = 6.96$ LAE (magenta circle; Iye et al. 2006), the $z = 7.22$ LAE (cyan circle; Shibuya et al. 2012), and from LAEz7p7 suggest such a trend between $z \simeq 7$ and 7.7. Note that the above LAEs at $z = 6.96$ and 7.22 were discovered in much larger survey volumes.

The combination of this work and previous work enables us to put a more stringent constraint on the Lyα LF. Clément et al. (2012) did not find any $z \simeq 7.7$ LAEs in their survey. Although Hibon et al. (2010) found seven LAE candidates, none of their five brightest candidates were confirmed by follow-up spectroscopy, as mentioned by Clément et al. (2012). A conservative summary is that, in the above three surveys, including Krug et al. (2012), there is no $z \simeq 7.7$ LAE with Lyα emission higher than 10^{-17} erg s^{-1} cm^{-2} ($L \geqslant 6.9 \times 10^{42}$ erg s^{-1}). If we assume a non-evolution of Lyα LF from $z \simeq 6.5$ to 7.7, we expect to find $\sim$6 LAEs down to the above flux limit, based on the LF of Kashikawa et al. (2011). The probability of finding zero LAEs is 0.0025, under the assumption of a Poisson distribution. By combining the three surveys, the uncertainty due to cosmic variance has been largely reduced, and the Poisson statistical uncertainty dominates the uncertainty of the LF. Note that there is a discrepancy between the Kashikawa et al. (2011) LFs and the Hu et al. (2010) LFs, but they are roughly consistent at the brightest end. The non-detection in the three studies translates to an upper limit of the bright-end Lyα LF at $z \simeq 7.7$. The black circle in Figure 4 represents this upper limit (corresponding to the detection of one LAE). This limit is much stronger than that from LAEz7p7 alone. It shows a rapid evolution of the Lyα LF at the bright end from $z \simeq 6.5$ to 7.7: the upper limit of the $z \simeq 7.7$ LF is a factor of six times lower than the $z \simeq 6.5$ LF.

The decline of the Lyα LF does not necessarily mean an increasing fraction of neutral IGM since this could also be caused by the intrinsic luminosity and/or density evolution of LAEs (e.g., Jensen et al. 2013). With limited information, we cannot rule out any intrinsic evolution. In particular, we know that the UV LF of LBGs evolves at this redshift (e.g., Bouwens et al. 2012; Oesch et al. 2012). However, such a rapid change of the LF in Figure 4 is not likely to be due mainly to intrinsic evolution because the time interval between $z = 6.5$ and 7.7 is only 165 Myr, and the physical properties of LAEs evolve slowly at $3 \leqslant z \leqslant 6$ (e.g., Malhotra et al. 2012; Jiang et al. 2013). On the other hand, the increasing optical depth of the Lyα forest toward $z > 6$ quasars indicates a rapid rise in the IGM neutral fraction. Because of radiative transfer effects, the Lyα emission line is largely shaped by its environment and more attenuated by a higher fraction of neutral hydrogen (e.g., Malhotra & Rhoads 2004; Zheng et al. 2010; Dijkstra et al. 2011). At $z \simeq 6.5$, the neutral fraction is still very small ($\ll$10%; Fan et al. 2006), yet it may already cause strong suppression on the Lyα emission (Figure 4). A recently discovered quasar at $z = 7.08$ (Mortlock et al. 2011) was estimated to have a neutral fraction of $\sim$10% in the surrounding IGM (Bolton et al. 2011). We thus expect a much higher neutral fraction of the IGM at $z \simeq 7.7$ than that at $z \simeq 6.5$. Therefore, the Lyα emission of $z \simeq 7.7$ LAEs would be strongly suppressed, which is broadly consistent with the observational trend in Figure 4.

Finally, we estimate the fraction of observed Lyα flux that is reduced by neutral IGM at $z \simeq 7.7$. We assume a pure luminosity evolution of the Lyα LF from $z \simeq 6.5$ to 7.7. We also assume that such evolution was caused by the IGM. The black line in Figure 4 shows the evolved $z \simeq 6.5$ LF matched to the LF upper limit (black circle) at $z \simeq 7.7$. We find that the Lyα luminosity at $z \simeq 7.7$ is reduced by at least a factor of two compared to that at $z \simeq 6.5$.

Support for this work was provided by NASA through Hubble Fellowship grant HST-HF-51291.01 awarded by STScI, which is operated by the Association of Universities for Research in Astronomy, Inc., for NASA, under contract NAS 5-26555. F.B., X.F., and I.D.M. acknowledge supports from NSF grants AST 08-06861 and 11-07682.

Facility: LBT (LUCI)

REFERENCES

Ageorges, N., Seifert, W., Jütte, M., et al. 2010, Proc. SPIE, 7735, 53
Bian, F., Fan, X., Bechtold, J., et al. 2010, ApJ, 725, 1877
Bolton, J. S., Haehnelt, M. G., Warren, S. J., et al. 2011, MNRAS, 416, L70
Bouwens, R. J., Illingworth, G. D., Oesch, P. A., et al. 2012, ApJL, 752, L5
Carilli, C. L., Wang, R., Fan, X., et al. 2010, ApJ, 714, 834
Clément, B., Cuby, J.-G., Courbin, F., et al. 2012, A&A, 538, A66
Dijkstra, M., Mesinger, A., & Wyithe, J. S. B. 2011, MNRAS, 414, 2139
Fan, X., Carilli, C. L., & Keating, B. 2006, ARA&A, 44, 415
Hibon, P., Cuby, J.-G., Willis, J., et al. 2010, A&A, 515, 97
Hu, E. M., Cowie, L. L., Barger, A. J., et al. 2010, ApJ, 725, 394
Iye, M., Ota, K., Kashikawa, N., et al. 2006, Natur, 443, 186
Jensen, H., Laursen, P., Mellema, G., et al. 2013, MNRAS, 428, 1366
Jiang, L., Egami, E., Mechtley, M., et al. 2013, ApJ, in press (arXiv:1303.0024)
Kashikawa, N., Shimasaku, K., Matsuda, Y., et al. 2011, ApJ, 734, 119
Kelson, D. D. 2003, PASP, 115, 688
Komatsu, E., Smith, K. M., Dunkley, J., et al. 2011, ApJS, 192, 18
Krug, H. B., Veilleux, S., Tilvi, V., et al. 2012, ApJ, 745, 122
Malhotra, S., & Rhoads, J. E. 2004, ApJL, 617, L5
Malhotra, S., Rhoads, J. E., Finkelstein, S. L., et al. 2012, ApJL, 750, L36
McGreer, I. D., Mesinger, A., & Fan, X. 2011, MNRAS, 415, 3237
Mesinger, A., & Haiman, Z. 2007, ApJ, 660, 923
Mortlock, D. J., Warren, S. J., Venemans, B. P., et al. 2011, Natur, 474, 616
Oesch, P. A., Bouwens, R. J., Illingworth, G. D., et al. 2012, ApJ, 759, 135
Ota, K., Richard, J., Iye, M., et al. 2012, MNRAS, 423, 2829
Ouchi, M., Shimasaku, K., Furusawa, H., et al. 2010, ApJ, 723, 869
Pirzkal, N., Rothberg, B., Ryan, R., et al. 2013, arXiv:1304.4594
Rhoads, J. E., Hibon, P., Malhotra, S., Cooper, M., & Weiner, B. 2012, ApJL, 752, L28
Shibuya, T., Kashikawa, N., Ota, K., et al. 2012, ApJ, 752, 114
Shimasaku, K., Kashikawa, N., Doi, M., et al. 2006, PASJ, 58, 313
Stark, D. P., Ellis, R. S., & Ouchi, M. 2011, ApJL, 728, L2
Taniguchi, Y., Ajiki, M., Nagao, T., et al. 2005, PASJ, 57, 165
Tilvi, V., Rhoads, J. E., Hibon, P., et al. 2010, ApJ, 721, 1853
Treu, T., Trenti, M., Stiavelli, M., Auger, M. W., & Bradley, L. D. 2012, ApJ, 747, 27
Zheng, Z., Cen, R., Trac, H., & Miralda-Escudé, J. 2010, ApJ, 716, 574